Forest Ecology and Management 491 (2021) 119157

Contents lists available at ScienceDirect

Forest Ecology and Management

journal homepage: www.elsevier.com/locate/foreco

Inter-specific transpiration differences between aspen, spruce, and pine in a sky-island ecosystem of the North American Great Basin

Xinsheng Liu [a,b], Franco Biondi [a,*]

[a] DendroLab, Department of Natural Resources and Environmental Science, University of Nevada, Reno, NV 89557, USA
[b] College of Tourism and Geography, Jiujiang University, East Qianjin Road No. 551, Jiujiang 332005, China

ARTICLE INFO

Keywords:
Sap flow
Populus tremuloides
Picea engelmannii
Pinus flexilis
Canopy conductance
NevCAN

ABSTRACT

Semiarid forests may face future challenges because of climate change-exacerbated soil droughts. Because the risk and rate of tree mortality from soil drying can vary widely between co-occurring species, inter-specific differences in tree response need to be evaluated for designing science-driven best-management strategies specifically tailored to iconic sky-island ecosystems. We analyzed sap flow of quaking aspen (*Populus tremuloides*), Engelmann spruce (*Picea engelmannii*), and limber pine (*Pinus flexilis*) for five consecutive years (2014–2018) at a remote, high-elevation site in the North American Great Basin. Our results revealed species-specific responses of sap flow to declining soil moisture. For quaking aspen, multi-year sap-flow trajectories mimicked growing-season depletion of soil moisture. Ample cool-season precipitation in 2017 diminished the summer drought impact on sap flow of Engelmann spruce and limber pine, indicating that the two conifers could tap a deeper soil water reservoir than the deciduous species. Since species-specific transpiration response to soil droughts was driven by shifting precipitation regimes, our findings suggest niche partitioning in the rhizosphere among coexisting tree species. In addition, spruce and pine rapidly downregulated canopy conductance with decreasing soil water availability, whereas aspen canopy conductance was insensitive to soil drying. This physiological characteristic allows quaking aspen to maximize resource acquisition when growing conditions are favorable, but poses a risk of hydraulic failure and subsequent mortality under soil drying. Overall, we found contrasting hydrological niches and physiological strategies between co-occurring tree species in semiarid, high-elevation ecosystems. We also emphasize the value of long-term, in-situ observations to determine species-specific susceptibility to environmental changes in remote mountain areas.

1. Introduction

Subalpine sky islands are isolated mountain ranges surrounded by lowland desert valleys in regions where strong elevation gradients determine rapid changes in climate and vegetation (Debano et al., 1995). This globally unique ecosystem is sensitive to climate changes and their interactions with wildfire (Iniguez et al., 2015), insect outbreaks (O'Connor et al., 2015), and human disturbances (Poulos et al., 2013). Drought in western North American forests leads to depletion in soil water availability, which has been tied to large-scale tree die-off (Cook et al., 2015; Goulden and Bales, 2019). Not only because of differential physiological response to soil drying, but also because of the shift in hydrological patterns and associated timing of soil drying (Szejner et al., 2020), the risk and rate of tree mortality varies widely among co-occurring tree species (Ganey and Vojta, 2011; Kane et al., 2014; Smith and Smith, 2005). Such species-dependent responses may affect vegetation composition and its associated ecosystem goods and services, hence they need to be evaluated in order to design science-driven best-management strategies. In-depth understanding of the interspecific differences in tree transpiration response to soil drying is still limited in sky-island ecosystems (Liu and Biondi, 2020), even though it is a premise to sustainable management schemes under changing climatic conditions in semiarid regions (del Campo et al., 2017; Loehle et al., 2016).

Sap flow measurements have been applied to quantify water relations and assess the physiological response of mature trees to soil drying in temperate (Brinkmann et al., 2016; Dietrich et al., 2019; Meinzer et al., 2013; Peters et al., 2019; Zweifel et al., 2009) and tropical (Kume et al., 2007) environments, with a growing interest in water-limited forests (Brito et al., 2015; Du et al., 2011; Pataki et al., 2000;

* Corresponding author.
E-mail address: fbiondi@unr.edu (F. Biondi).

https://doi.org/10.1016/j.foreco.2021.119157
Received 31 December 2020; Accepted 8 March 2021

Poyatos et al., 2008; Song et al., 2020). In many studies, transpiration reduction in response to soil drying differed among coexisting tree species. Species-specific drought sensitivity can be partly explained by different resistance to embolism in stems and/or roots, and by stomatal control of leaf water use, which in turn is determined by leaf and wood traits (leaf size and density, leaf conductance, and wood density), as well as hydraulic traits (hydraulic conductance and conduit size) (Adams et al., 2017; Choat et al. 2012; Martin-StPaul et al., 2017). Differences in rooting system and access to soil water pools can also be involved (Ripullone et al., 2020). In the western United States, water isotopic ratios have shown that conifers often depend primarily on winter precipitation sourced from deep soils (Hu et al., 2010; Martin et al., 2018; Roberts et al., 2004), but trembling aspen relies on summer rains from relatively shallow soil layers throughout the growing season (Anderegg et al., 2013). Although species-specific soil water niches were reported in two western conifers (Meinzer et al., 2007), to date, linkages between species-specific hydrological responses to soil drought and depth-specific variations in soil moisture remain unclear in sky-island forests. Such knowledge helps with predicting how trees may respond to hydroclimatic conditions created by shifting precipitation regimes in the western United States (Pederson et al., 2011).

Long-term adjustments in tree water use are reflected by changes in the leaf area to sapwood area ratio (Poyatos et al., 2007), but stomatal adjustments are considered the main physiological mechanism for regulating transpiration, and respond rapidly to adverse conditions in the atmosphere and soil (Klein, 2014; Martin-StPaul et al., 2017; McDowell et al., 2008). While stomatal response to atmospheric drought has been emphasized (but see Garcia-Forner et al., 2016; Peters et al., 2019), there is evidence for sensitivity of stomata to soil drought (Bonal et al., 2000; Liu and Biondi, 2020; Zhao et al., 2013). Rainfall manipulations and consequent changes in soil moisture conditions in mature forests (Grossiord et al., 2018; He et al., 2020; Leo et al., 2014) have shown that sap flow sensitivity, hence transpiration responses, can substantially differ among species (Leo et al., 2014). Prolonged exposure of roots to dry soil could lead to the synthesis of abscisic acid (Bartlett et al., 2012), which would induce stomatal closure (Comstock, 2002). Therefore, species-specific stomatal sensitivity to decreasing soil water availability may play an essential role in driving sap flow response to soil drought.

Hydroclimate variability in the western US has included a severe multi-year drought in 2012–2015 followed by exceptionally wet conditions in 2016–2017 (Wang et al., 2017). The 2012–2015 drought was associated with widespread forest die-offs that have been spatially and temporally linked with multi-year deep soil drying (Goulden and Bales, 2019). A unique opportunity to investigate the transpiration response of Great Basin sky-island tree species to such extreme climate episodes was available through the Nevada Climate-ecohydrological Assessment Network (NevCAN; Mensing et al., 2013). In the current study, our main goal was to test for species-specific patterns, and therefore we addressed the following questions: (1) was inter-specific variability of sap flow decline in response to soil drought connected with depth-specific variations in soil moisture?; (2) did cool- and warm-season precipitation influence growing-season tree transpiration?; (3) was canopy conductance of evergreen and deciduous species equally sensitive to soil drought? We pursued our objectives by analyzing field measurements of tree-level sap flow, as well as in-situ atmospheric and soil variables, conducted at sub-hourly time steps over five years (2014–2018) on three co-dominant species at a high-elevation remote mountain site.

2. Material and methods

2.1. Study site and environmental data

Field measurements were collected at a subalpine stand (39.009°N, 114.309°W, 3063 m. a.s.l.) on the eastern slope of the Snake Range in central-eastern Nevada. The study area is part of the Nevada Climate-ecohydrological Assessment Network (NevCAN), a long-term elevational and latitudinal mountain observatory for evaluating climatic effects on ecohydrological processes (Mensing et al., 2013). Each NevCAN site is equipped with a standard weather station, as well as additional automated sensors to measure sub-hourly changes in the atmosphere, soil, and vegetation – see Liu and Biondi, 2020, for details on NevCAN sensors and the variables they measure. In particular, soil sensors were installed at 10- and 20-cm depths to capture differences between, respectively, shallow and deep soil layers because of the overall rockiness of the study area, as was reported in previously published analyses of soil properties at NevCAN sites (Johnson et al., 2014, 2016). A map and an annotated photograph of the study site are included in the graphical abstract.

Environmental data recorded at the site during 2014–2018 were obtained from the Western Regional Climate Center (https://wrcc.dri.edu/GBtransect/). These numerical records were supplemented by 10-minute instrumental observations downloaded from the NevCAN database (ftp://sensor.nevada.edu/) as well as by snapshots taken at regular intervals by the webcam installed on the weather tower, which are also publicly available from the NevCAN database. Vapor pressure deficit (VPD, hPa) was computed as the difference between saturation vapor pressure (e_s, hPa) and actual vapor pressure (e_a, hPa), which was calculated using10-minute records of air temperature (T_a, ^{0}C) and relative humidity (RH, %) according to Jones (1992):

$$\mathrm{VPD} = e_s - e_a = (1 - \mathrm{RH}/100) \times 6.1078 \times \exp[(17.27 \times \mathrm{T_a})/(\mathrm{T_a} + 237.3)] \quad (1)$$

Our study site is located on the east slope of the Snake Range, within Great Basin National Park, in a relatively open and mixed stand dominated by Engelmann spruce (*Picea engelmannii* Parry ex Engelm.), quaking aspen (*Populus tremuloides Michx.*), and limber pine (*Pinus flexilis* E. James), with sparse or absent understory. Bedrock consists of till derived from quartzite, shale, and argillite, and soils are classified as loamy-skeletal, mixed, superactive xeric haplocryolls (Johnson et al., 2014). According to data recorded by the NevCAN weather station, and downloaded directly as 10-minute records from the NevCAN database (ftp://sensor.nevada.edu/), annual mean temperature varied little (<0.18 °C) from year to year, with an average of 2.6 ± 0.1 °C. The months of July (14.3 ± 1.2 °C) and December (–6.6 ± 1.4 °C) were the warmest and coldest ones, respectively. Annual total precipitation, which was defined using the water year (i.e., the 12 months from previous-calendar-year October through current-calendar-year September), averaged 523 ± 107 mm, 74% of which was received during the October–May period. Water-year precipitation reached a maximum in 2017 (704 mm; 35% above average) and a minimum in 2018 (409 mm; 22% below average).

Much longer, albeit interpolated rather than in-situ, instrumental records of precipitation and temperature are available from the public-domain version of the Parameter-Regression at Independent-Slopes Model (PRISM) dataset (Daly et al., 2008). Monthly values during 1895–2019 for the 4-km grid cell containing the study site were downloaded and used to represent the annual cycle in terms of total precipitation and mean temperature. We also calculated water-year, cool season (October–May), and growing season (June–September) precipitation totals, and used their empirical distribution and time-series features to evaluate if 2014–2018 were either dry or wet years.

2.2. Sap flow measurements

Sap flow in 2014–2018 was continuously measured by Granier-type thermal dissipation sensors (TDP30, Dynamax, Houston, Texas, USA) (Granier, 1987). In total, eight mature trees (3 quaking aspens, 3 Engelmann spruces and 2 limber pines) with no obvious damages were selected for sap flow measurements. Average stem diameter at breast height (DBH) of instrumented trees was 24 ± 3 cm for quaking aspen, 50 ± 21 cm for Engelmann spruce, and 53 ± 12 cm for limber pine, and the

average height was 9 ± 0 m, 12 ± 3 m and 11 ± 1 m, respectively. Selected trees represented the variability of stem size under natural conditions, which ensured the close coupling between the canopy of instrumented trees and the atmosphere. Each probe consists of a pair of needles (30-mm length and 1.2-mm diameter) equipped with a copper-constantan thermocouple inserted in an aluminum sleeve. The upper needle contained a set of wires continuously heated with a power of 0.15–0.20 W, whereas the lower needle measured ambient sapwood temperature and served as a reference. Previous studies have indicated that sapwood of quaking aspen, Engelmann spruce, and limber pine generally spans >30 mm from the outer edge of the bark (Anderegg et al., 2014; Liu and Biondi, 2020), hence the 30-mm-long needles rested within the active sapwood. Sensors were installed at breast height on the north-facing side of the tree trunk to diminish possible radiation effects on sap flow (Wieser et al., 2014). After some surface bark (approximately 1.5 cm × 1.5 cm) was carefully peeled off, the pair of needles was radially inserted approximately 15 cm apart from each other. To insulate from rain infiltration, and to avoid thermal influences from solar radiation, sensors were greased with waterproof silicone and shielded with aluminum box-covers.

Temperature differences between the heated and the reference needles were recorded every 30 s, and averages were stored on a CR1000 data logger with AM16/32 multiplexer (Campbell Scientific Inc. USA) at 10-min intervals. Using the empirical equation established by Granier (1987), temperature differences were converted to sap flux density, as follows:

$$F_{di} = 0.0119[(\Delta T_{max} - \Delta T)/\Delta T]^{1.231} \quad (2)$$

where F_{di} (g cm^{-2} s^{-1}) is the sap flux density of tree i, ΔT (°C) is the temperature difference when sap flow was occurring, and ΔT_{max} (°C) is the maximum value of ΔT recorded at night when sap flow approaches zero. At high elevations, nighttime vapor pressure deficits are commonly low and nighttime patterns of between-needle temperature are balanced, indicating that the recharge of stem water storage has completed. Therefore, ΔT_{max} was determined for every night and acted as a reference for the next day (Liu et al., 2016; Lu et al., 2004; Wieser et al., 2014).

Sap flux density of quaking aspen during the periods of leaf development and leaf senescence was not corrected. Instead, we determined time intervals when leaves were fully expanded by visually inspecting weekly images captured by the NevCAN webcam. Leaves were completely expanded by 24 June in every year, whereas the date of leaf senescence varied between 8 September (2018) and 15 September (2014–2017; Fig. S1). These year-specific phenological leaf stages were used to restrict sap flow values of quaking aspen to periods with fully expanded leaves.

Sap flux density (F_d, g cm^{-2} d^{-1}) was summed within a day (06:00–20:00 local time) to reduce the potential effects of internal stem water capacitance on the response of transpiration to soil moisture (Oren et al., 1998; Wieser et al., 2014). Because absolute tree water use can vary with morphological and physiological parameters (e.g. tree size, leaf area, and wood anatomy), F_d was normalized as follows. During each growing season (May–October) in 2014–2018, maximum F_d was determined for every instrumented tree, and normalized F_d was defined as the ratio between daily sap flux density and maximum F_d throughout the growing season (Brinkmann et al., 2016; Dietrich et al., 2019; Du et al., 2011; Liu et al., 2016; Wieser et al., 2014). Normalized tree values were averaged to yield mean normalized F_d by species.

2.3. Analysis of environmental relationships

The relationship between normalized F_d and daily mean soil moisture was modeled by the following exponential saturation function:

$$F_d = y_0 + a[1 - exp(-b\ \mathrm{SM})] \quad (3)$$

where SM is daily mean soil moisture (SM, %), a, b and y_0 are fitting parameters. We also estimated canopy conductance (G_c) according to an inverted Penman-Monteith equation (Köstner et al., 1992) under the assumption that the forest canopy is aerodynamically well coupled to the atmosphere. The formula takes the following form:

$$G_c = k(F_d/\mathrm{VPD}) \quad (4)$$

where F_d is whole-tree sap flux density (g cm^{-2} d^{-1}), VPD is vapor pressure deficit (kPa), and k is a conductance coefficient derived from water density, the gas constant for water vapor, and air temperature. Eq. (4) requires that there is no difference between VPD and the leaf-to-air vapor pressure deficit, that no vertical profile exists through the canopy, and that stem water storage above the sap flow measurement position can be neglected (Ewers and Oren, 2000). Such conditions are generally satisfied in aspen and conifer forests (Ewers et al., 2005).

A simplified relative mean daily canopy conductance (g_c) was also calculated as the ratio of normalized F_d and VPD (Du et al., 2011; Wieser et al., 2014; Liu and Biondi, 2020). To account for differences in canopy conductance, g_c values were further standardized to the individual-specific maximum canopy conductance (Pappas et al., 2018; Peters et al., 2019). Normalized g_c and G_c were finally averaged by species to investigate its sensitivity to soil drying and radiation. Species-specific relationships of normalized g_c or G_c with soil moisture and radiation were modeled by simple regression. A $\log_{10}$ transformation was applied to g_c, G_c, and soil moisture in order to obtain linear relationships. Differences in slope among species (g_c or G_c as a dependent variable, soil moisture as a covariate, and species as a grouping variable) were tested by analysis of covariance (ANCOVA; McDonald, 2014).

Tree (sap flow and canopy conductance) responses to soil drought were separately analyzed by year using days without rainfall when daily mean solar radiation exceeded 4.0 kW hr m^{-2} and daily mean vapor pressure deficit exceeded 0.5 kPa (Ewers et al., 2005; Liu and Biondi, 2020; Meinzer et al., 2013). Rainy and overcast days were excluded because those conditions will lead to low sap flow rates and unrealistic high values of canopy conductance that are unrelated to soil moisture. We used repeated measures analysis of variance (ANOVA; McDonald, 2014) to examine effects of species and year on sap flow and canopy conductance. All statistical analyses were performed using SPSS 22.0 for Windows (SPSS Inc., USA).

3. Results

3.1. Environmental variability

During the warm season (June–September), PRISM data showed slightly warmer (3–6% higher temperature) and wetter (11–51% higher precipitation) conditions than the NevCAN station, although the year-to-year changes followed identical patterns (Table 1). Cool-season (October–May) precipitation was widely different between PRISM data and values obtained from the NevCAN database (Table 1). Given that NevCAN records provided by the Western Regional Climate Center (https://wrcc.dri.edu/cgi-bin/rawMAIN.pl?idnep7) appeared even less reliable (e.g., total October–May precipitation in some years was lower than that for June–September; *data not shown*), we decided to use PRISM precipitation data in our subsequent analyses.

Based on PRISM records and their summary representation in a Walter-Lieth diagram of precipitation and temperature regimes (Fig. S2a), summer drought is usually absent at this high-elevation site. By considering the full PRISM length (1896–2019), it was possible to place the years 2014–2018 in a longer climate perspective. October–May precipitation in those years ranged from 320 to 664 mm, amounts which bracketed a substantial portion of the entire distribution (Fig. S2b). Similarly, June–September precipitation ranged from 62 to 287 mm, which also spanned the majority of the entire distribution (Fig. S2b). Growing-season precipitation was about average in 2015 and

Table 1
Summary of environmental variables[a] for growing-season (June–September) and cool-season (October–May) measured at the NevCAN station (with comparisons to PRISM data[b]).

Months	Variable	Year				
		2014	2015	2016	2017	2018
Jun-Sep	T_a (°C)	11.29	12.07	12.14	11.41	13.00
	T_aP (°C)	11.60	12.38	12.48	12.08	13.43
	T_s (°C)	10.97	11.74	12.04	11.24	13.55
	R_a (kW hr m^{-2})	5.07	4.89	5.37	4.70	4.82
	VPD (kPa)	0.77	0.89	1.01	0.83	1.05
	Prec (mm)	245	131	56	119	41
	PrecP (mm)	287	161	62	160	62
	SM_{10} (%)	17.28	15.12	12.10	14.20	10.64
	SM_{20} (%)		13.96	10.89	11.22	8.47
Oct-May	Prec (mm)	317	375	369	585	368
	PrecP (mm)	463	432	623	664	320

[a] T_a = mean daily air temperature; T_s = mean daily soil temperature at 10-cm depth; R_a = mean daily solar radiation; VPD = mean daily vapor pressure deficit; Prec = total precipitation; SM_{10} and SM_{20} = mean daily soil moisture at 10-cm and 20-cm depth, respectively.
[b] T_aP = mean monthly air temperature from PRISM; PrecP = total precipitation from PRISM.

2017, below average in 2016 and 2018, and well above average in 2014 (Table 1 and Fig. S2c). Cool-season precipitation did not follow those year-to-year patterns, and was above average in 2016 and 2017, but below average in 2014, 2015, and especially in 2018 (Table 1 and Fig. S2c).

The 2018 and 2014 growing seasons had not only low and high precipitation, but also the respectively highest and lowest temperatures (in both air and soil) and vapor pressure deficits (Table 1 and Fig. S3a, b). Growing-season total solar radiation varied little among years (the inter-annual variation was < 0.67 kW hr m^{-2}). Overall, summer water stress reached a high peak in 2018 and a low one in 2014. Despite low cool-season precipitation in 2014, that year was characterized by abundant summer precipitation (Table 1 and Fig. S3c). As a consequence, different seasonal patterns of soil moisture were observed among years. Water content in shallow soil (10-cm depth, SM_{10}) during May and early June was about 1.8 times higher in 2015–2018 than in 2014, but during the rest of the 2014 growing-season SM_{10} remained above 12%, while it dropped below that value in 2015–2018 (Fig. S3c). Sporadic summer rainfall combined with high vapor pressure deficit resulted in a progressive soil moisture decline and substantial soil drying every year from 2015 to 2018. In 2016 and 2018, soil moisture at 20 cm depth (SM_{20}) during June–September dropped down to 5% (Fig. S3c).

3.2. Sap flow and its relation to soil drought

Sap flow differed significantly among species and years (Table 2). For all tree species, sap flow remained high and showed no declining trend over the 2014 growing season (Fig. 1a), most likely because of the wet summer and relatively high soil moisture (cf. Table 1 and Fig. S3c). In 2015 and 2017, sap flow of all tree species started to decrease in late August, and stayed at low values (except for quaking aspen) until mid-September, when soil rewetting occurred (Fig. 1b, d). Earlier (around late July) decrease in sap flow was observed in 2016 and 2018, most likely because of dry summers and severe soil drying (Fig. 1c, e).

Table 2
Summary of repeated measures ANOVA for the response of sap flow and canopy conductance to species, year, and their interaction during 2014–2018.

Response variable	Factor	*df*	*F*-test	*P*-value
Sap flow	Species	2	55.68	<0.001
	Year	4	28.36	<0.001
	Species × year	8	11.38	<0.001
Canopy conductance	Species	2	304.14	<0.001
	Year	4	11.88	<0.001
	Species × year	8	6.01	<0.001

The late-season decline in sap flow relative to the growing seasonal maximum varied among species and years (Figs. 1 and 2). In 2015, 2016 and 2018, limber pine and Engelmann spruce reduced sap flow by 84–87% and 77–86%, respectively. These two conifer species showed the lowest sap flow reduction (66% for limber pine and 63% for Engelmann spruce) in 2017, when cool-season precipitation was above average and growing season precipitation was about average (cf. Table 1). Quaking aspen exhibited a lower reduction in sap flow than the conifers during the growing seasons of 2017 (47%) and 2015 (57%), whereas it was comparable to both spruce and pine in 2016 and 2018 (77%). Differences in late-season sap flow reduction among species were related to year-specific seasonal maxima rather than to absolute sap flow values. Across years, the late-season down-regulation in sap flow relative to the growing seasonal maximum of quaking aspen was negatively correlated with June–September precipitation ($r = -0.92$, $P = 0.082$), whereas the two conifers showed a significant negative correlation with October–May precipitation ($r = -0.90$, $P = 0.002$; *data not shown*).

Sap flow and soil moisture were closely related for all three species, except in 2014 (Fig. S4). During the 2015–2018 growing seasons, sap flow decreased with increasing soil drought (Figs. 2 and S4d–o), showing a nonlinear relation with soil moisture at 20 cm (R^2 = 0.34–0.87 and all $P < 0.001$; Fig. 2) and at 10 cm depth (R^2 = 0.35–0.86 and all $P < 0.001$; Fig. S4d–o). In those same periods, warm-season rainfall events (July 19–22 in 2015, June 28 - July 3 in 2016, July 23–28 in 2017, and July 8–14 in 2018) led to an increase in soil moisture (Fig. S3c). Soil rewetting induced a fast increase in sap flow of quaking aspen, which persisted for four weeks (Fig. 3a). The two conifers, by contrast, exhibited a smaller response to soil rewetting, which rapidly subsided one week later (Fig. 3a). Canopy conductance of quaking aspen post-rewetting was generally comparable to that during soil rewetting, whereas the two conifers downregulated substantially after rewetting (Fig. 3b).

3.3. Canopy conductance response to soil drought

Differences in canopy conductance among species and years were found to be statistically significant (Table 2). Quaking aspen displayed contrasting canopy conductance in terms of seasonal dynamics and magnitudes when compared to limber pine and Engelmann spruce (Fig. S5). Across years, canopy conductance of the conifer species varied widely, reaching a peak in the early (before mid-June in 2015–2018) or in the late (after mid-September in 2014) growing seasons, i.e. when soil moisture was favorable. In contrast, there was no large seasonal variability in canopy conductance of quaking aspen, which consistently maintained higher values than the conifers during the growing season.

For all species and years, the response of canopy conductance to soil moisture was nonlinear, and could best be described using a logarithmic transformation (Fig. 4). Canopy conductance of quaking aspen generally showed almost no decline with decreasing soil moisture, whereas limber pine and Engelmann spruce displayed a strong downregulation of canopy conductance with increasing soil drought (Fig. 4 and Table S1). There was no significant relationship between canopy conductance and solar radiation, except for aspen in 2014 (Fig. S6). Across years and soil depths, the g_c–SM slopes did not differ significantly between Engelmann spruce and limber pine ($P > 0.05$; Table S1). In general, the g_c–SM slopes for quaking aspen were lower than those of Engelmann spruce and limber pine ($P < 0.05$; Table S1). To avoid biasing the results, we also restricted the analysis of conifer data to the annual periods with fully expanded leaves of quaking aspen, and it was still possible to identify species-specific canopy conductance sensitivity to soil drought, and a lower ability of quaking aspen for stomatal adjustment under soil drying (Fig. S7 and Table S2).

After combining data of normalized daily mean canopy conductance

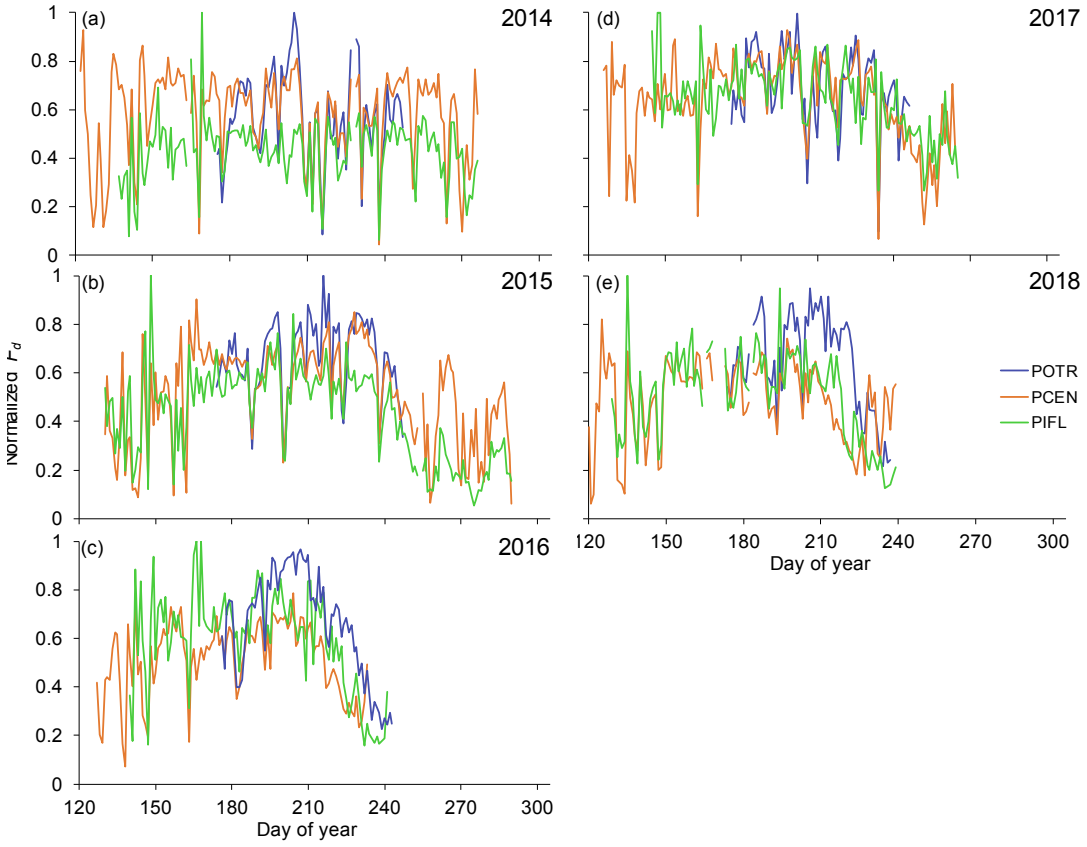

Fig. 1. Normalized daily sap flux density (Normalized F_d) for *Populus tremuloides* (POTR), *Picea engelmannii* (PCEN) and *Pinus flexilis* (PIFL) in years 2014–2018. Note that POTR sap flow was only shown for days with full leaf expansion and no obvious leaf senescence (see text for details).

(g_c) for all years (Fig. 5), both conifers showed a positive connection between canopy conductance and soil moisture, with no significant difference in g_c–SM_{20} slopes between spruce and pine ($F = 3.29$, $P = 0.061$). Such connection was absent for aspen, as the slope in Fig. 5 was itself not significant, and therefore significantly lower than those for spruce and pine. The linearized equations (in log-scale; see Fig. 5) used to represent the linkage between canopy conductance and soil moisture could be expressed as a power relationship for each tree species, as follows:

$$g_c = 0.344\ SM_{20}^{0.1102} \quad (Populus\ \ tremuloides) \tag{5}$$

$$g_c = 0.031\ SM_{20}^{0.6497} \quad (Picea\ \ engelmannii) \tag{6}$$

$$g_c = 0.016\ SM_{20}^{0.8382} \quad (Pinus\ \ flexilis) \tag{7}$$

Daily mean canopy conductance (G_c) of all species linearly declined with decreasing soil moisture, and the G_c–SM_{20} slopes for spruce ($F = 28.95$, $P < 0.001$) and pine ($F = 43.85$, $P < 0.001$) were significantly higher than that for aspen (Fig. S8).

4. Discussion

4.1. Differential sap flow response to soil drying among co-occurring species

Drought-induced forest die-off has been reported for many forest ecosystems (Allen et al., 2010), including those in western North America. While large-scale tree mortality has been connected to deep soil drying during the 2012–2015 California drought (Goulden and Bales, 2019), information is still needed on how coexisting tree species may respond differently to water stress, especially in sky-island environments. Our study area did not experience exactly the same timing and intensity of dry and wet periods recorded elsewhere in the western US (Wang et al., 2017), since the lowest cool-season precipitation was recorded in 2018, and 2014 was characterized by the highest growing-season rainfall (Table 1 and Fig. S2c). Yet field conditions over the five years of our study captured most of the long-term seasonal variability of precipitation (Table 1 and Fig. S2b).

Sap flow data highlighted species-specific reduction of transpiration in response to declining soil moisture (Figs. 2 and S4). Our observations were in agreement with the notion that broad-leaved tree species are generally less resistant to drought than co-occurring coniferous species (Brinkmann et al., 2016; Pataki et al., 2000). Although such differences among species are often linked to hydraulic and functional traits (Adams et al., 2017; Choat et al. 2012), our data revealed that species-specific decline in sap flow was not uniform every year, and depended on depth-specific soil moisture and its recharge by previous cool-season or current warm-season precipitation.

Variable year-to-year summer rainfall led to different seasonal dynamics of soil moisture depletion (Fig. S3c). Overall, the multi-year trajectories and magnitudes of decline in sap flow for quaking aspen closely tracked growing-season depletion of soil moisture (Figs. 1, 2 and S4). Therefore, interannual variability of sap flow decline in response to soil drying suggested that quaking aspen relies primarily on shallower water sources when compared to the conifer species. The root system of quaking aspen is relatively shallow, and the majority of functional lateral roots can extend over 30 m into open areas (Burns and Honkala, 1990). Stable isotopic analysis has been used to suggest that quaking aspen mainly taps water from shallow ground layers, with little plasticity (i.e., ability to switch water source) during drought stress (Anderegg et al., 2013).

Increased cool-season precipitation (October–May) normally

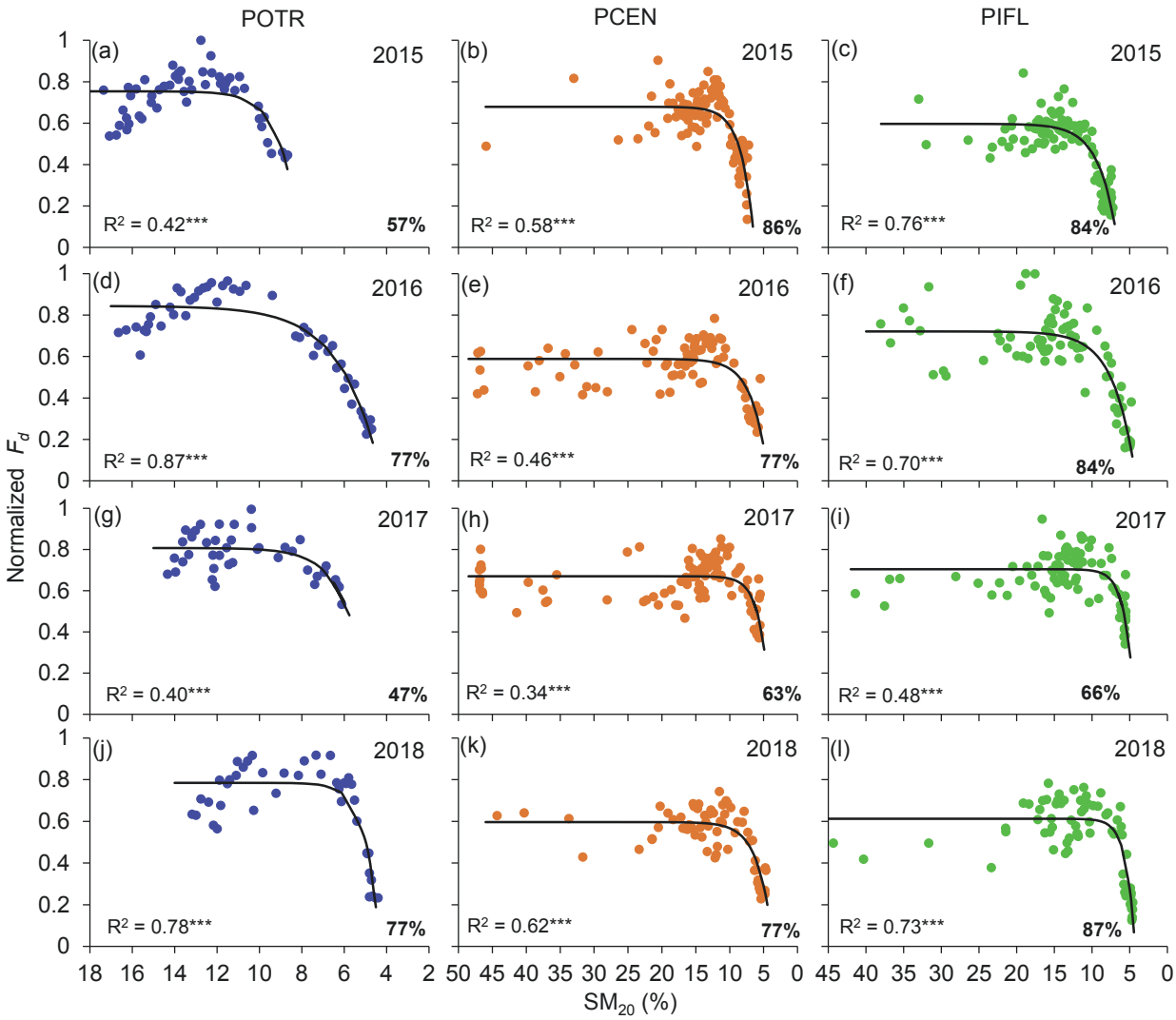

Fig. 2. Relationships between normalized daily sap flux density (Normalized F_d) and daily mean soil water content at 20 cm depth (SM_{20}) for *Populus tremuloides* (POTR), *Picea engelmannii* (PCEN) and *Pinus flexilis* (PIFL) in years 2015–2018. An exponential saturation function was fit to the data, and both the model R^2 and the model significance (*** = *P*-value < 0.001) are shown. Only days without rainfall when daily mean solar radiation exceeded 4.0 kW hr m^{-2} and daily mean vapor pressure deficit exceeded 0.5 kPa were included in the analysis. The percentage in each inset indicates the late-season decline in sap flow relative to the growing seasonal maximum. Note the x-axis values decrease from left to right.

translates into enhanced soil moisture at deeper levels during the growing season, thereby mitigating the drought impact on summertime transpiration (Brito et al., 2015; Liu and Biondi, 2020). This occurred in 2017, the wettest winter, when spruce and pine both exhibited the least reduction in sap flow compared to other years with relatively dry winters (Table 1, Figs. 2 and S4). Average June–September rainfall in 2015 and 2017 did not consistently correspond to a decline in conifer sap flow during the summer (Table 1, Figs. 2 and S4), and stable isotopic studies have pointed to a reliance on water from cool-season snowmelt for Engelmann spruce (Hu et al., 2010) and limber pine (Roberts et al., 2004). Although we could not directly determine soil water uptake depths, the multi-year dynamics of sap flow response suggested that conifers could tap a deeper soil water reservoir than the deciduous species in order to withstand summer drought.

Conifer sap flow was maintained over the 2014 growing season so that no declining trend was detected (Figs. 1a and S4a–c). This pattern could be explained either by recharge of deep soil moisture from abundant summer rain (Table 1 and Fig. S3c) or by a shift to shallow water uptake. In water-limited environments, some coniferous species are able to in fact modify water sources under natural and experimental droughts (Grossiord et al., 2017; Martin et al., 2018). Also, in 2014 growing season sap flow was relatively low compared to other years for all three species, and especially for limber pine (Fig. 1a), possibly because of higher competition among species.

All species displayed a nonlinear sap flow decline with decreasing soil moisture in 2015–2018 (Figs. 2 and S4). Moreover, the critical soil moisture threshold at which sap flow started to decline was roughly identical across years and species. Downregulation of sap flow began when soil moisture dropped below 10%, but at different soil depths: 10 cm for quaking aspen (Fig S4), and 20 cm for Engelmann spruce and limber pine (Fig. 2). The patterns seen in conifer species at this site replicates what we observed in a nearby high-elevation stand, where the 10% soil moisture threshold at 20-cm depth significantly reduced transpiration sensitivity of limber and bristlecone pine (*Pinus longaeva*) to atmospheric evaporative demand (Liu and Biondi, 2020). Such soil moisture threshold further explained varying timings of sap flow decline in 2015–2018 and no sap flow decline in 2014 (Figs. S3c and 1).

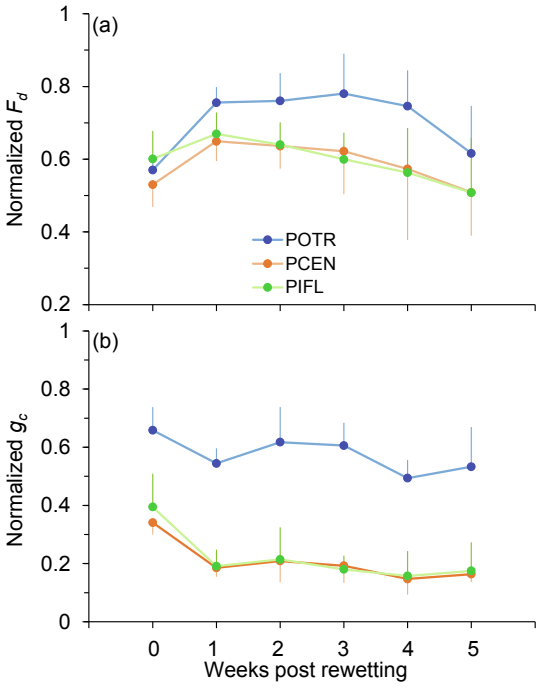

Fig. 3. Weekly means of normalized daily (a) sap flux density (Normalized F_d) and (b) canopy conductance (Normalized g_c) for *Populus tremuloides* (POTR), *Picea engelmannii* (PCEN) and *Pinus flexilis* (PIFL) during and after soil rewetting. Data points are averages of four representative rewetting events during the 2015–2018 growing seasons (see text for details), and bars represent one standard deviation.

4.2. Species-specific sensitivity of canopy conductance to soil drought

Categorizing plants into isohydric and anisohydric water-use strategies, often inferred from stomatal sensitivity to atmospheric evaporative demand, has been proposed as a key mechanism underlying drought-induced tree mortality (Klein, 2014; McDowell et al., 2008). However, iso- and aniso-hydric behavior can be more dependent on the environment where the plant lives than due to inherent properties of the species (Hochberg et al., 2018). The two co-occurring conifers at our study site downregulated stomatal conductance with decreasing soil moisture, whereas aspen exhibited insignificant stomatal adjustment in response to soil drought (Figs. 4, 5, S8 and Table S1). In other words, our observations indicate that soil drought exerts a weak control over canopy conductance of quaking aspen compared with two conifers in a sky-island ecosystem. This insensitive stomatal behavior to soil drying is in accordance with leaf-level measurements, in which quaking aspen exhibited little stomatal control over water loss, and had open stomata during severe droughts (Tobiessen and Kana, 1974; Kaufmann, 1982).

Divergent stomatal behavior under soil drought involves sensing mechanisms and processes driving the stomatal adjustment in response to changing soil water availability (Brodribb and McAdam, 2013). Chemical root-to-shoot signaling has been shown to trigger responses in guard cell membrane channels and transporters, which will induce a loss in guard cell turgor and thereby stomata closure in water-stressed gymnosperms (Schachtman and Goodger, 2008). Under severe soil drying, this mechanism should induce a lower minimum conductance for conifers, which facilitates the maintenance of hydraulic integrity and thereby reduces the risk of hydraulic failure and mortality (Blackman et al., 2019; Hammond and Adams, 2019). At the same time, this mechanism usually results in a delay of stomata reopening after rewatering, and therefore implies a slower post-drought transpiration recovery of gymnosperms (i.e. low capacity to regain pre-drought transpiration rates; Brodribb and McAdam, 2013). If acute drought occurs, negative effects of soil moisture-dependent stomata regulation on transpiration recovery may persist and severely affect tree internal carbon balances (Galiano et al., 2011; McDowell et al., 2008), inducing long-term legacy effects and triggering mortality in conifers (DeSoto et al., 2020).

Insensitive stomatal response of quaking aspen to soil drought suggests that the species may respond passively through changes in leaf water potential induced by vapor pressure deficit (Brodribb and McAdam, 2013; Loewenstein and Pallardy, 1998). Soil moisture-independent stomatal regulation confers quaking aspen the ability to immediately reopen stomata as soon as soil is rehydrated by a rainfall

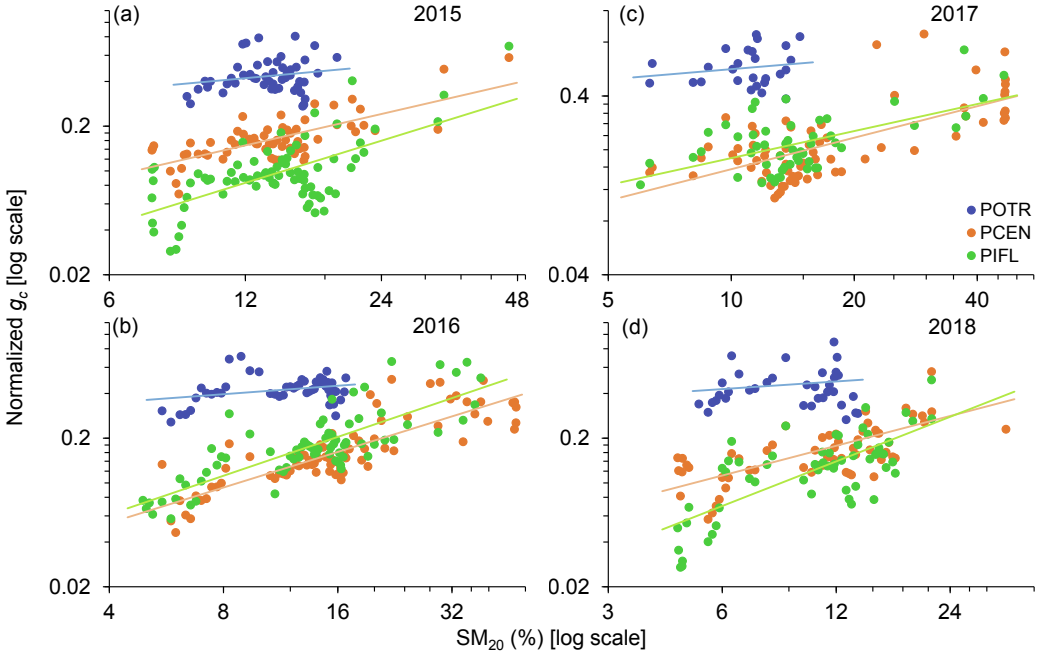

Fig. 4. Response of normalized daily mean canopy conductance (g_c; log-scale) to soil moisture at 20 cm depth (SM_{20}, log-scale) for *Populus tremuloides* (POTR), *Picea engelmannii* (PCEN) and *Pinus flexilis* (PIFL) in years 2015–2018 (see Table S1). Note the different scales of g_c and soil moisture between years.

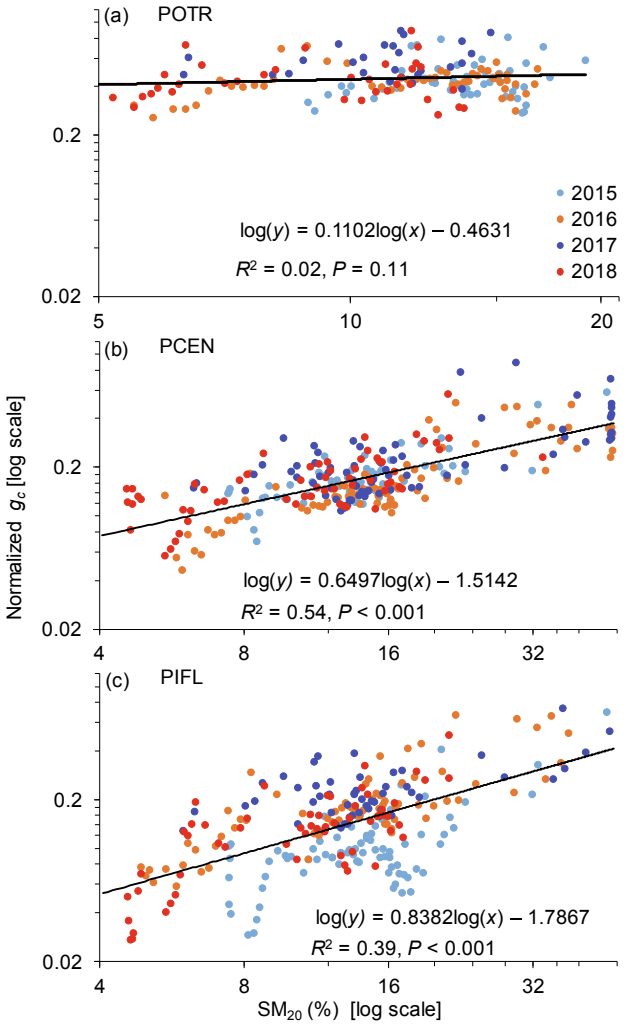

Fig. 5. Response of normalized daily mean canopy conductance (g_c; log-scale) to soil moisture at 20 cm depth (SM_{20}, log-scale) for *Populus tremuloides* (POTR), *Picea engelmannii* (PCEN) and *Pinus flexilis* (PIFL). The vertical axis (for g_c) is the same across species, while the horizontal axis (for SM_{20}) is the same for spruce and pine but covers a smaller range of values for aspen.

event. This strategy reflects the "fast" ecological trait of this species, i.e. being able to maintain higher water conductance and to acquire resources during temporarily favorable conditions (Pappas et al., 2018). On the other hand, limited stomata adjustments and relatively higher minimum conductance under severe soil drying suggest that quaking aspen should approach hydraulic failure and mortality more rapidly than the coexisting conifers (Blackman et al., 2019; Hammond and Adams, 2019).

5. Conclusions

Thanks to a unique dataset of continuous, multi-year, sub-hourly sap flow and environmental observations, we uncovered species-specific transpiration responses in a sky-island ecosystem. Seasonal transpiration decline in response to soil drought was connected with soil moisture in the upper soil layer for quaking aspen, whereas ample cool-season precipitation, and therefore deeper soil water, reduced summer transpiration decline of Engelmann spruce and limber pine. Our results imply niche partitioning of the rhizosphere in water-limited forests, which may diminish drought impacts on the ecosystem as a whole (Grossiord et al., 2014). Further, canopy conductance of quaking aspen was not sensitive to reduced soil water availability compared to the conifers, which potentially increases the threat of hydraulic failure and subsequent mortality for quaking aspen. These findings provide a physiological basis for understanding species-specific risk of drought-induced die-offs among co-occurring tree species in semiarid, high-elevation ecosystems, hence they have a direct connection with designing science-driven best-management conservation strategies specifically tailored to such fascinating areas in a changing world.

Declaration of Competing Interest

The authors declare that they have no known competing financial interests or personal relationships that could have appeared to influence the work reported in this paper.

Acknowledgements

This work was funded, in part, by the US National Science Foundation under grant AGS-P2C2-1502379 to F. Biondi and E. Ziaco. F. Biondi was also supported, in part, by the US National Science Foundation under grant AGS-P2C2-1903561. X. Liu was funded by the National Natural Science Foundation of China (41961008) and by the Natural Science Foundation of Jiangxi, China (20192BAB203021). X. Liu is grateful for the support from the China Scholarship Council (201908360038). We thank S. Strachan for NevCAN maintenance. The views and conclusions contained in this document are those of the authors and should not be interpreted as representing the opinions or policies of the funding agencies and supporting institutions.

Appendix A. Supplementary material

Supplementary data to this article can be found online at https://doi.org/10.1016/j.foreco.2021.119157.

References

Adams, H.D., Zeppel, M.J.B., Anderegg, W.R.L., Hartmann, H., Landhäusser, S.M., Tissue, D.T., Huxman, T.E., Hudson, P.J., Franz, T.E., Allen, C.D., Anderegg, L.D.L., Barron-Gafford, G.A., Beerling, D.J., Breshears, D.D., Brodribb, T.J., Bugmann, H., Cobb, R.C., Collins, A.D., Dickman, L.T., Duan, H.L., Ewers, B.E., Galiano, L., Galvez, D.A., Garcia-Forner, N., Gaylord, M.L., Germino, M.J., Gessler, A., Hacke, U. G., Hakamada, R., Hector, A., Jenkins, M.W., Kane, J.M., Kolb, T.E., Law, D.J., Lewis, J.D., Limousin, J.M., Love, D.M., Macalady, A.K., Martinez-Vilalta, J., Mencuccini, M., Mitchell, P.J., Muss, J.D., O'Brien, M.J., O'Grady, A.P., Pangle, R.E., Pinkard, E.A., Piper, F.I., Plaut, J.A., Pockman, W.T., Quirk, J., Reinhardt, K., Ripullone, F., Ryan, M.G., Sala, A., Sevanto, S., Sperry, J.S., Vargas, R., Vennetier, M., Way, D.A., Xu, C.G., Yepez, E.A., McDowell, N.G., 2017. A multispecies synthesis of physiological mechanisms in drought-induced tree mortality. Nat. Ecol. Evol. 1, 1285–1291. https://doi.org/10.1038/s41559-017-0248-x.

Allen, C.D., Macalady, A.K., Chenchouni, H., Bachelet, D., McDowell, N., Vennetier, M., Kitzberger, T., Rigling, A., Breshears, D.D., Hogg, E.H., Gonzalez, P., Fensham, R., Zhang, Z., Castro, J., Demidova, N., Lim, J.-H., Allard, G., Running, S.W., Semerci, A., Cobb, N., 2010. A global overview of drought and heat-induced tree mortality reveals emerging climate change risks for forests. For. Ecol. Manag. 259, 660–684. https://doi.org/10.1016/j.foreco.2009.09.001.

Anderegg, L.D.L., Anderegg, W.R.L., Abatzoglou, J., Hausladen, A.M., Berry, J.A., 2013. Drought characteristics' role in widespread aspen forest mortality across Colorado, USA. Glob. Chang. Biol. 19, 1526–1537. https://doi.org/10.1111/gcb.12146.

Anderegg, W.R.L., Anderegg, L.D.L., Berry, J.A., Field, C.B., 2014. Loss of whole-tree hydraulic conductance during severe drought and multi-year forest die-off. Oecologia 175, 11–23. https://doi.org/10.1007/s00442-013-2875-5.

Bartlett, M.K., Scoffoni, C., Sack, L., 2012. The determinants of leaf turgor loss point and prediction of drought tolerance of species and biomes: a global meta-analysis. Ecol. Lett. 15, 393–405. https://doi.org/10.1111/j.1461-0248.2012.01751.x.

Blackman, C.J., Creek, D., Maier, C., Aspinwall, M.J., Drake, J.E., Pfautsch, S., O'Grady, A., Delzon, S., Medlyn, B.E., Tissue, D.T., Choat, B., 2019. Drought response strategies and hydraulic traits contribute to mechanistic understanding of plant dry-down to hydraulic failure. Tree Physiol. 39, 910–924. https://doi.org/10.1093/treephys/tpz016.

Bonal, D., Barigah, T.S., Granier, A., Guehl, J.M., 2000. Late-stage canopy tree species with extremely low $\delta^{13}C$ and high stomatal sensitivity to seasonal soil drought in the tropical rainforest of French Guiana. Plant Cell Environ. 23, 445–459. https://doi.org/10.1046/j.1365-3040.2000.00556.x.

Brinkmann, N., Eugster, W., Zweifel, R., Buchmann, N., Kahmen, A., 2016. Temperate tree species show identical response in tree water deficit but different sensitivities in

sap flow to summer soil drying. Tree Physiol. 36, 1508–1519. https://doi.org/10.1093/treephys/tpw062.
Brito, P., Lorenzo, J.R., González-Rodríguez, Á.M., Morales, D., Wieser, G., Jiménez, M. S., 2015. Canopy transpiration of a semi arid *Pinus canariensis* forest at a treeline ecotone in two hydrologically contrasting years. Agric. For. Meteorol. 201, 120–127. https://doi.org/10.1016/j.agrformet.2014.11.008.
Brodribb, T.J., McAdam, S.A.M., 2013. Abscisic Acid Mediates a Divergence in the Drought Response of Two Conifers. Plant Physiol. 162, 1370–1377. https://doi.org/10.1104/pp.113.217877.
Burns, R.M., Honkala, B.H., 1990. Silvics of North America. United States Department of Agriculture.
Choat, B., Jansen, S., Brodribb, T.J., Cochard, H., Delzon, S., Bhaskar, R., Bucci, S.J., Feild, T.S., Gleason, S.M., Hacke, U.G., Jacobsen, A.L., Lens, F., Maherali, H., Martínez-Vilalta, J., Mayr, S., Mencuccini, M., Mitchell, P.J., Nardini, A., Pittermann, J., Pratt, R.B., Sperry, J.S., Westoby, M., Wright, I.J., Zanne, A.E., 2012. Global convergence in the vulnerability of forests to drought. Nature 491, 752–755. https://doi.org/10.1038/nature11688.
Comstock, J.P., 2002. Hydraulic and chemical signalling in the control of stomatal conductance and transpiration. J. Exp. Bot. 367, 195–200. https://doi.org/10.1093/jexbot/53.367.195.
Cook, B.I., Ault, T.R., Smerdon, J.E., 2015. Unprecedented 21st century drought risk in the American Southwest and Central Plains. Sci. Adv. 1, e1400082. https://doi.org/10.1126/sciadv.1400082.
Daly, C., Halbleib, M., Smith, J.I., Gibson, W.P., Doggett, M.K., Taylor, G.H., Curtis, J., Pasteris, P.P., 2008. Physiographically sensitive mapping of temperature and precipitation across the conterminous United States. Int. J. Climatol. 28, 2031–2064. https://doi.org/10.1002/joc.1688.
DeBano, L.H., Ffolliott, P.H., Ortega-Rubio, A., Gottfried, G.J., Hamre, R.H., Carleton, B., 1995. Biodiversity and Management of the Madrean Archipelago: The Sky Islands of Southwestern United States and Northwestern Mexico. In: Rocky Mountain Forest and Range Experiment Station, General Technical Report. USDA Forest Service, General Technical Report, RM-GTR-264, Tucson, AZ.
del Campo, A.D., Sonzález-Sanchis, M., Lidón, A., García-Prats, A., Lull, C., Bautista, I., Ruíz-Pérez, G., Francés, F., 2017. Ecohydrological-based forest management in semi-arid climate. In: Křeček, J., Haigh, M., Hofer, T., Kubin, E., Promper, C. (Eds.), Ecosystem Services of Headwater Catchments. Springer, Cham.
DeSoto, L., Cailleret, M., Sterck, F., Jansen, S., Kramer, K., Robert, E.M.R., Aakala, T., Amoroso, M.M., Bigler, C., Camarero, J.J., Čufar, K., Gea-lzquierdo, G., Gillner, S., Haavik, L.J., Heres, A., Kane, J.M., Kharuk, V.I., Kitzberger, T., Klein, T., Levanič, T., Linares, J.C., Mäkinen, H., Oberhuber, W., Papadopoulos, A., Rohner, B., Sangüesa-Barreda, G., Stojanovic, D.B., Suárez, L.M., Villalba, R., Martínez-Vilalta, J., 2020. Low growth resilience to drought is related to future mortality risk in trees. Nat. Commun. 11, 545. https://doi.org/10.1038/s41467-020-14300-5.
Dietrich, L., Delzon, S., Hoch, G., Kahmen, A., 2019. No role for xylem embolism or carbohydrate shortage in temperate trees during the severe 2015 drought. J. Ecol. 107, 334–349. https://doi.org/10.1111/1365-2745.13051.
Du, S., Wang, Y.L., Kume, T., Zhang, J.G., Otsuki, K., Yamanaka, N., Liu, G.B., 2011. Sapflow characteristics and climatic responses in three forest species in the semiarid Loess Plateau region of China. Agric. For. Meteor. 15, 1–10. https://doi.org/10.1016/j.agrformet.2010.08.011.
Ewers, B.E., Oren, R., 2000. Analyses of assumptions and errors in the calculation of stomatal conductance from sap flux measurements. Tree Physiol. 20, 579–589. https://doi.org/10.1093/treephys/20.9.579.
Ewers, B.E., Gower, S.T., Bond-Lamberty, B., Wang, C.K., 2005. Effects of stand age and tree species composition on transpiration and canopy conductance of boreal forests. Plant Cell Environ. 28, 660–678. https://doi.org/10.1111/j.1365-3040.2005.01312.x.
Galiano, L., Martínez-Vilalta, J., Lloret, F., 2011. Carbon reserves and canopy defoliation determine the recovery of Scots pine 4 yr after a drought episode. New Phytol. 190, 750–759. https://doi.org/10.1111/j.1469-8137.2010.03628.x.
Ganey, J.L., Vojta, S.C., 2011. Tree mortality in drought-stressed mixed-conifer and ponderosa pine forests, Arizona, USA. For. Ecol. Manage. 261, 162–168. https://doi.org/10.1016/j.foreco.2010.09.048.
Garcia-Forner, N., Adams, H.D., Sevanto, A., Collins, A.D., Dickman, L.T., Hudson, P.J., Zeppel, M.J.B., Jenkins, M.W., Powers, H., Martínez-Vilalta, J., McDowell, N.G., 2016. Responses of two semiarid conifer tree species to reduced precipitation and warming reveal new perspectives for stomatal regulation. Plant Cell Environ. 39, 38–49. https://doi.org/10.1111/pce.12588.
Goulden, M.L., Bales, R.C., 2019. California forest die-off linked to multi-year deep soil drying in 2012–2015 drought. Nat. Geosci. 12, 632–637. https://doi.org/10.1038/s41561-019-0388-5.
Granier, A., 1987. Evaluation of transpiration in a Douglas-fir stand by means of sap flow measurements. Tree Physiol. 3, 309–320. https://doi.org/10.1093/treephys/3.4.309.
Grossiord, C., Granier, A., Ratcliffe, S., Bouriaud, O., Bruelheide, H., Chećko, E., Forrester, D.I., Dawud, S.M., Finér, L., Pollastrini, M., Scherer-Lorenzen, M., Valladares, F., Bonal, D., Gessler, A., 2014. Tree diversity does not always improve resistance of forest ecosystems to drought. Proc. Natl. Acad. Sci. U. S. A. 111, 14812–14815. https://doi.org/10.1073/pnas.1411970111.
Grossiord, C., Sevanto, S., Dawson, T.E., Adams, H.D., Collins, A.D., Dickman, L.T., Newman, B.D., Stockton, E.A., McDowell, N.G., 2017. Warming combined with more extreme precipitation regimes modifies the water sources used by trees. New Phytol. 213, 584–596. https://doi.org/10.1111/nph.14192.
Grossiord, C., Sevanto, S., Limousin, J.M., Meir, P., Mencuccini, M., Pangle, R.E., Pockman, W.T., Salmon, Y., Zweifel, R., McDowell, N.G., 2018. Manipulative experiments demonstrate how long-term soil moisture changes alter controls of plant water use. Environ. Exp. Bot. 152, 19–27. https://doi.org/10.1016/j.envexpbot.2017.12.010.
Hammond, W.M., Adams, H.D., 2019. Dying on time: traits influencing the dynamics of tree mortality risk from drought. Tree Physiol. 39, 906–909. https://doi.org/10.1093/treephys/tpz050.
He, Q., Yan, M., Miyazawa, Y., Chen, Q., Cheng, R., Otsuki, K., Yamanaka, N., Du, S., 2020. Sap flow changes and climatic responses over multiple-year treatment of rainfall exclusion in a sub-humid black locust plantation. For. Ecol. Manage. 457, 117730. https://doi.org/10.1016/j.foreco.2019.117730.
Hochberg, U., Rockwell, F.E., Holbrook, N.M., Cochard, H., 2018. Iso/Anisohydry: A Plant-Environment Interaction Rather Than a Simple Hydraulic Trait. Trends Plant Sci. 23, 112–120. https://doi.org/10.1016/j.tplants.2017.11.002.
Hu, J., Moore, D.J.P., Burns, S.P., Monson, R.K., 2010. Longer growing seasons lead to less carbon sequestration by a subalpine forest. Glob. Change Biol. 16, 771–783. https://doi.org/10.1111/j.1365-2486.2009.01967.x.
Iniguez, J.M., Swetnam, T.W., Baisan, C.H., 2015. Fire history and moisture influences on historical forest age structure in the sky islands of southern Arizona, USA. J. Biogeogr. 43, 85–95. https://doi.org/10.1111/jbi.12626.
Johnson, B.G., Verburg, P.S.J., Arnone III, J.A., 2014. Effects of climate and vegetation on soil nutrients and chemistry in the Great Basin studied along a latitudinal-elevational climate gradient. Plant Soil 382, 151–163. https://doi.org/10.1007/s11104-014-2144-3.
Johnson, B.G., Verburg, P.S.J., Arnone III, J.A., 2016. Plant species effects on soil nutrients and chemistry in arid ecological zones. Oecologia 182, 299–317. https://doi.org/10.1007/s00442-016-3655-9.
Jones, H.G., 1992. Plants and Microclimate: A Quantitative Approach to Environmental Plant Physiology, second ed. Cambridge University Press, Cambridge.
Kane, J.M., Kolb, T.E., McMillin, J.D., 2014. Stand-scale tree mortality factors differ by site and species following drought in southwestern mixed conifer forests. For. Ecol. Manage. 330, 171–182. https://doi.org/10.1016/j.foreco.2014.06.042.
Kaufmann, M.R., 1982. Leaf conductance during the final season of a senescing aspen branch. Plant Physiol. 70, 655–657. https://doi.org/10.1104/pp.70.3.655.
Klein, T., 2014. The variability of stomatal sensitivity to leaf water potential across tree species indicates a continuum between isohydric and anisohydric behaviours. Funct. Ecol. 28, 1313–1320. https://doi.org/10.1111/1365-2435.12289.
Köstner, B.M.M., Schulze, E.D., Kelliher, F.M., Hollinger, D.Y., Byers, J.N., Hunt, J.E., McSeveny, T.M., Meserth, R., Weir, P.L., 1992. Transpiration and canopy conductance in a pristine broad-leaved forest of *Nothofagus*: an analysis of xylem sap flow and eddy correlation measurements. Oecologia 91, 350–359. https://doi.org/10.1007/BF00317623.
Kume, T., Takizawa, H., Yoshifuji, N., Tanaka, K., Tantasirin, C., Tanaka, N., Suzuki, M., 2007. Impact of soil drought on sap flow and water status of evergreen trees in a tropical monsoon forest in northern Thailand. For. Ecol. Manage. 238, 220–230. https://doi.org/10.1016/j.foreco.2006.10.019.
Leo, M., Oberhuber, W., Schuster, R., Grams, T.E.E., Matyssek, R., Wieser, G., 2014. Evaluating the effect of plant water availability on inner alpine coniferous trees based on sap flow measurements. Eur. J. For. Res. 133, 691–698. https://doi.org/10.1007/s10342-013-0697-y.
Liu, X., Nie, Y., Luo, T., Yu, J., Shen, W., Zhang, L., 2016. Seasonal shift in climatic limiting factors on tree transpiration: Evidence from sap flow observations at alpine treelines in southeast Tibet. Front. Plant Sci. 7, 1018. https://doi.org/10.3389/fpls.2016.01018.
Liu, X., Biondi, F., 2020. Transpiration drivers of high-elevation five-needle pines (*Pinus longaeva* and *Pinus flexilis*) in sky-island ecosystems of the North American Great Basin. Sci. Total Environ. 739, 139861. https://doi.org/10.1016/j.scitotenv.2020.139861.
Loehle, S., Idso, C., Wigley, T.B., 2016. Physiological and ecological factors influencing recent trends in United States forest health responses to climate change. For. Ecol. Manage. 363, 179–189. https://doi.org/10.1016/j.foreco.2015.12.042.
Loewenstein, N.J., Pallardy, S.G., 1998. Drought tolerance, xylem sap abscisic acid and stomatal conductance during soil drying: a comparison of young plants of four temperate deciduous angiosperms. Tree Physiol. 18, 421–430. https://doi.org/10.1093/treephys/18.7.421.
Lu, P., Urban, L., Zhao, P., 2004. Granier's Thermal Dissipation Probe (TDP) method for measuring sap flow in trees: Theory and practice. Acta Bot. Sin. 46, 631–646.
Martin, J., Looker, N., Hoylman, Z., Jencso, K., Hu, J., 2018. Differential use of winter precipitation by upper and lower elevation Douglas fir in the Northern Rockies. Glob. Change Biol. 24, 5607–5621. https://doi.org/10.1111/gcb.14435.
Martin-StPaul, N., Delzon, S., Cochard, H., 2017. Plant resistance to drought depends on timely stomatal closure. Ecol. Lett. 20, 1437–1447. https://doi.org/10.1111/ele.12851.
McDonald, J.H., 2014. Handbook of Biological Statistics, 3 ed. Sparky House Publishing, Baltimore, MD.
McDowell, N., Pockman, W.T., Allen, C.D., Breshears, D.D., Cobb, N., Kolb, T., Plaut, J., Sperry, J., West, A., Williams, D.G., Yepez, E.A., 2008. Mechanisms of plant survival and mortality during drought: why do some plants survive while others succumb to drought? New Phytol. 178, 719–739. https://doi.org/10.1111/j.1469-8137.2008.02436.x.
Meinzer, F.C., Warren, J.M., Brooks, J.R., 2007. Species-specific partitioning of soil water resources in an old-growth Douglas-fir–western hemlock forest. Tree Physiol. 27, 871–880. https://doi.org/10.1093/treephys/27.6.871.
Meinzer, F.C., Woodruff, D.R., Eissenstat, D.M., Lin, H.S., Adams, T.S., McCulloh, K.A., 2013. Above- and belowground controls on water use by trees of different wood types in an eastern US deciduous forest. Tree Physiol. 33, 345–356. https://doi.org/10.1093/treephys/tpt012.

Mensing, S., Strachan, S., Arnone, J., Fenstermaker, L., Biondi, F., Devitt, D., Johnson, B., Bird, B., Fritzinger, E., 2013. A network for observing Great Basin climate change. Eos Trans. Am. Geophys. Union 94, 105–106. https://doi.org/10.1002/2013EO110001.

O'Connor, C.D., Lynch, A.M., Falk, D.A., Swetnam, T.W., 2015. Post-fire forest dynamics and climate variability affect spatial and temporal properties of spruce beetle outbreaks on a Sky Island mountain range. For. Ecol. Manage. 336, 148–162. https://doi.org/10.1016/j.foreco.2014.10.021.

Oren, R., Philips, N., Katul, G., Ewers, B.E., Pataki, D.E., 1998. Scaling xylem sap flux and soil water balance and calculating variance. A method for partitioning water flux in forests. Ann. For. Sci. 55, 191–216. https://doi.org/10.1051/forest:19980112.

Pappas, C., Matheny, A.M., Baltzer, J.L., Barr, A.G., Black, T.A., Bohrer, G., Detto, M., Maillet, J., Roy, A., Sonnentag, O., Stephens, J., 2018. Boreal tree hydrodynamics: asynchronous, diverging, yet complementary. Tree Physiol. 38, 953–964. https://doi.org/10.1093/treephys/tpy043.

Pataki, D.E., Oren, R., Smith, W.K., 2000. Sap flux of co-occurring species in a western subalpine forest during seasonal soil drought. Ecology 81, 2557–2566. https://doi.org/10.1890/0012-9658(2000)081[2557:SFOCOS]2.0.CO;2.

Pederson, G.T., Gray, S.T., Woodhouse, C.A., Betancourt, J.L., Fagre, D.B., Littell, J.S., Watson, E., Luckman, B.H., Graumlich, L.J., 2011. The unusual nature of recent snowpack declines in the North American cordillera. Science 543, 332–336. https://doi.org/10.1126/science.1201570.

Peters, R.L., Speich, M., Pappas, C., Kahmen, A., von Arx, G., Pannatier, E.G., Steppe, K., Treydte, K., Stritih, A., Fonti, P., 2019. Contrasting stomatal sensitivity to temperature and soil drought in mature alpine conifers. Plant Cell Environ. 42, 1674–1689. https://doi.org/10.1111/pce.13500.

Poulos, H.M., Villanueva Díaz, J., Cerano Paredes, J., Camp, A.E., Gatewood, R.G., 2013. Human influences on fire regimes and forest structure in the Chihuahuan Desert Borderlands. Forest Ecol. Manag. 298, 1–11. https://doi.org/10.1016/j.foreco.2013.02.014.

Poyatos, R., Martínez-Vilalta, J., Čermák, J., Ceulemans, R., Granier, A., Irvine, J., Köstner, B., Lagergren, F., Meiresonne, L., Zadezhdina, N., Zimmermann, R., Llorens, P., Mencuccini, M., 2007. Plasticity in hydraulic architecture of scots pine across Eurasia. Oecologia 153, 245–259. https://doi.org/10.1007/s00442-007-0740-0.

Poyatos, R., Llorens, P., Piñol, J., Rubio, C., 2008. Response of Scots pine (*Pinus sylvestris* L.) and pubescent oak (*Quercus pubescens* Willd.) to soil and atmospheric water deficits under Mediterranean mountain climate. Ann. For. Sci. 65, 306. https://doi.org/10.1051/forest:2008003.

Ripullone, F., Camarereo, J.J., Colangelo, M., Voltas, J., 2020. Variation in the access to deep soil water pools explains tree-to-tree differences in drought-triggered dieback of Mediterranean oaks. Tree Physiol. 40, 591–604. https://doi.org/10.1093/treephys/tpaa026.

Roberts, L.M., Mcculley, R.L., Burke, I.C., Lauenroth, W.K., 2004. Indications of Deep Soil Water Usage by Limber Pine (*Pinus flexilis*) and Skunkbush Sumac (*Rhus aromatica*) in Northeastern Colorado: An Oxygen Isotope Study. Am. Midl. Nat. 152, 178–182 https://doi.org/10.1674.

Schachtman, D.P., Goodger, J.Q., 2008. Chemical root to shoot signaling under drought. Trends Plant Sci. 13, 281–287. https://doi.org/10.1016/j.tplants.2008.04.003.

Smith, A.E., Smith, F.W., 2005. Twenty-year change in aspen dominance in pure aspen and mixed aspen/conifer stands on the Uncompahgre Plateau, Colorado, USA. Forest Ecol. Manag. 213, 338–348. https://doi.org/10.1016/j.foreco.2005.03.018.

Song, L., Zhu, J., Zheng, X., Wang, K., Lü, L., Zhang, X., Hao, G., 2020. Transpiration and canopy conductance dynamics of *Pinus sylvestris* var. *mongolica* in its natural range and in an introduced region in the sandy plains of Northern China. Agric. For. Meteorol. 281, 107830. https://doi.org/10.1016/j.agrformet.2019.107830.

Szejner, P., Belmecheri, S., Ehleringer, J.R., Monson, R.K., 2020. Recent increases in drought frequency cause observed multi-year drought legacies in the tree rings of semi-arid forests. Oecologia 192, 241–259. https://doi.org/10.1007/s00442-019-04550-6.

Tobiessen, P., Kana, T.M., 1974. Drought-stress avoidance in three pioneer tree species. Ecology 55, 667–670. https://doi.org/10.2307/1935159.

Wang, S.Y.S., Yoon, J.-H., Becker, E., Gillies, R., 2017. California from drought to deluge. Nat. Clim. Change 7, 465–468. https://doi.org/10.1038/nclimate3330.

Wieser, G., Gruber, A., Oberhuber, W., 2014. Sap flow characteristics and whole-tree water use of *Pinus cembra* across the treeline ecotone of the central Tyrolean Alps. Eur. J. For. Res. 133, 287–295. https://doi.org/10.1007/s10342-013-0760-8.

Zhao, J., Hartmann, H., Trumbore, S., Ziegler, W., Zhang, Y., 2013. High temperature causes negative whole-plant carbon balance under mild drought. New Phytol. 200, 330–339. https://doi.org/10.1111/nph.12400.

Zweifel, R., Rigling, A., Dobbertin, M., 2009. Species-specific stomatal response of trees to drought a link to vegetation dynamics? J. Vegetation Sci. 20, 442–454. https://doi.org/10.1111/j.1654-1103.2009.05701.x.